ARTICLE

First Principles Study of Half-metallic Properties at MnSb/GaSb(001) Interface

Elmira Sartipi[a*], Alireza Hojabri[a], Arash Bouchani[b], Mohammad Homayion Shakib[a]

a. Physics Department, Islamic Azad University, Karaj Branch, Karaj, Iran
b. Physics Department, Islamic Azad University, Kermanshah Branch, Kermanshah, Iran

(Dated: Received on November 6, 2010; Accepted on January 10, 2011)

Density functional theory calculations are performed to study the structural, electronic and magnetic properties of hexagonal NiAs type and cubic zinc blende type MnSb structure and interface of zinc blende MnSb with GaSb(001). We used generalized gradiant approximation to calculate the exchange-correlation term in bulk and interface determination. The zinc blende structure of MnSb is found to be ferromagnetic half-metal with a total moment of 4 μ_B per formula unit. Results show that the half-metallicity character is preserved at MnSb/GaSb(001) interface. The magnetic moment of Mn atom in interface is reduced and the magnetic moment of the interface Sb atom is equal to the average of the corresponding bulk values in two sides of the interface. The band alignment properties are also computed and a rather large minority valance band offset of about 1.25 eV is obtained in this hetero-junction.

Key words: Spintronic, Surface, Interface, Density functional theory

I. INTRODUCTION

After the discovery of giant magneto resistance (GMR) by Fert *et al.* [1] and Grünberg *et al.* [2] in 1988, a new field in condensed matter, the magneto- or spinelectronics, have been evolved steadily. Because of the spin-dependent conductivity in these materials using ferromagnetic (FM) contacts as spin sources could be considered as a promising approach for this purpose. However Schmith *et al.* and Zhu *et al.* noticed that due to the conductivity mismatch at the FM metal/semiconductor interface, the measured spin polarization of the injected current would be very small [3, 4]. Half-metallic ferromagnets have been proposed as a possible solution for this serious obstacle and they could be considered as potential candidates for efficient spin injection into semiconductors [5]. The FM materials exhibit a metallic density of state (DOS) in one spin channel (usually majority spin) while there is a band gap around the Fermi level in the other spin channel, leading to 100% Fermi level spin polarization.

The most successful attempts have been done concerning the injection of spin-current from a dilute magnetic semiconductor such as GaMnAs, in which Mn atoms have substituted Ga atoms. Onhno *et al.* have used such contacts to inject spin-polarized electrons and holes into GaAs and obtained an efficiency of 90% spin-polarized current in GaAs [6]. On the other hand, existing magnetic semiconductors have a very low Curie temperature T_C. Other known half-metallic materials have been found such as CrO_2 and $La_{0.7}Sr_{0.3}MnO_3$ [7], which have practically 100% spin polarization at Fermi level at low temperature [8], but they also have low T_C too. Finally the half-metallic Heusler alloys such as NiMnSb [5, 9] are presented at T_C far above the room temperature, but their surface has not half-mettalic property [10]. It is difficult to control the stoichiometry of these surfaces experimentally [11]. However, it is highly desirable to explore new half-metallic ferromagnetic materials which are compatible with important III–V and II–VI semiconductors. For this purpose, a new class of half-metallic binary alloys with zincblende (ZB) structure was proposed. These materials are increasingly attracting attentions because of rather high T_C, large magnetic moment and good compatibility with conventional ZB semiconductors. These materials usually crystallize in NiAs type structure but first principles studies show that in the metastable ZB structure, they are FM half-metals. In order to stabilize ZB structure, thin films of these alloys have been grown on conventional ZB semiconductors. In this way, ZB phases of MnAs [12], CrAs [13, 14], CrSb [15], and CrTe [16, 17] have been successfully fabricated as nano dots, ultra thin film, and ultra thin layers in multi layers.

Later Pasket *et al.* theoretically predicted that the ZB MnSb phase is a robust half-metallic ferromagnrtic with a magnetic moment of 4.00 μ_B per unit formula [18]. A practical approach for stabilizing the MnSb compound in metastable ZB structure is the pseudo-

*Author to whom correspondence should be addressed. E-mail: elmira_s62@yahoo.com, Tel.: +98-261-4182300, FAX: +98-261-4182303

DOI:10.1088/1674-0068/24/02/155-161 ©2011 Chinese Physical Society

morphic growth of MnSb thin films on ZB semiconductors. The calculated lattice parameter of ZB MnSb is about 6.0 Å [19, 20], which has a negligible difference with the experimental lattice parameter of GaSb (6.1 Å). Recently the MnSb film layer has been grown under a semiconductor substrate such as InP and Si [21, 22]. Therefore ZB MnSb might be grown on ZB semiconductors such as GaSb. For practical purpose it is important to define whether or not the HM materials preserve the half-metallicity at thier interfaces. In this work, we have theoretically investigated the HM behaviors on the MnSb bulk and also MnSb/GaSb(001) interface by density functional-full potential computations.

II. COMPUTATIONAL METHOD

We used the FPLAPW+lo method implemented in the Wien2K package [23] within the spin-polarized density-functional theory (DFT), in which the exchange-correlation energy of electrons is described in the generalized gradient approximation (GGA) [24]. Relativistic effects are taken into account within the scalar approximation, neglecting the spin-orbit coupling. Basis functions, charge density, and potential are expanded inside muffin-tin spheres in combination with spherical harmonic functions with a cut-off $l_{\max}$=10. Moreover, we used a parameter $R_{\mathrm{MT}}K_{\max}$=8 in order to determine the matrix size, where $K_{\max}$ is the plane wave cut-off and R_{MT} is the smallest of all atomic sphere radii. For all atoms, R_{MT} was chosen as 2.2 a.u. In all our calculations we used a 8×8×1 mesh points for K-points in the Brillouin zone. The self-consistent calculations will be converged when the integrated charge difference per formula unit, $\int|\rho_n-\rho_{n-1}|\,\mathrm{d}r$, is less than 10^{-5}.

III. STRUCTURAL, ELECTRONIC, AND MAGNETIC PROPERTIES

A. Structural properties of bulk MnSb

The ground state structure of MnSb is a NiAs type structure with lattice constants a=7.84 Bohr and c=10.47 Bohr [18]. The lattice constant in ZB structure is also reported to be about 11.68 Bohr [19].

The structural properties of the NiAs and ZB type structure has also been calculated and listed in Table I. We use the FP method to calculate total energy of the NiAs and ZB structures at different volumes. By fitting the Murnaghan equation of states to obtain total energy-volume curves (Fig.1), it can be seen that with no compression or expansion, the NiAs structure is more stable than ZB structure. There is a phase transition from NiAs to ZB structure by −7.85 GPa pressure.

TABLE I The structural properties of FM state of MnSb in the NiAs and ZB type structure within GGA, lattice constant a in Bohr, axial ratio c/a, equilibrium volume V_0 in Bohr^3, magnetic moment M in μ_{B} , bulk module B in GPa, elastic constant parameters C_{ij} in GPa, cohesive energy E_{C} in Rydberg.

Structure	a	c/a	V_0	M	B	E_{C}	Ref.
NiAs	7.69	1.39	549.62	3.74	59.35	−0.87	
	7.84	1.40	585.10	3.83	44.90		[18]
	7.76	1.51	612.19			0.00	[19]
ZB	11.69		399.72	4.00	38.19	−0.80	
	11.68		398.60	4.00			[18]
	11.65		395.89	4.00			[19]

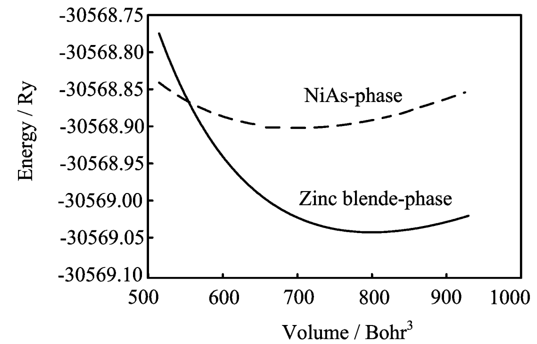

FIG. 1 Total energy versus volume MnSb in ZB and NiAs structure.

It can be concluded from these results that the obtained lattice constants and bulk modules by GGA methods are in good agreement with the other pervious works. Also, we have calculated the elastic constant for the ZB and NiAs type structure, cohesive energy and magnetic moment. Also, our calculated cohesive energy shows that the NiAs type structure is more stable than ZB type structure.

By using FP calculations the total magnetic moment in the ZB MnSb is 4.00 μ_{B}. This could be a signal for half-metallicity property of the ZB MnSb within GGA, in agreement with pervious calculations [19, 20]. In a FM half-metal, due to the presence of a gap at Fermi level of the minority states, there is no partially occupied minority state, leading to an integer number of spin down electrons in the system. Consequently the spin magnetic moment is also an integer number in a half-metal. This leads to a simple "rule of 8" [25]:

$$M_{\mathrm{tot}}=Z_{\mathrm{tot}}-8 \tag{1}$$

where 8 electrons contribute to bonding p-d bands and Z_{tot} is the total number of valance electrons. MnSb has 12 valance electrons in formula unit and so the total magnetic moment M_{tot} according to Eq.(1) should be 4 μ_{B}.

Following the method discussed in detail in Refs.[26, 27], we calculated the elastic constant $C_{11}-C_{12}$ and C_{44}

DOI:10.1088/1674-0068/24/02/155-161 ©2011 Chinese Physical Society

parameters from the volume-conserving orthorhombic strain tensor:

$$\begin{bmatrix} \delta & 0 & 0 \\ 0 & -\delta & 0 \\ 0 & 0 & \dfrac{\delta^2}{1-\delta^2} \end{bmatrix} \quad (2)$$

Application of this strain changes the total energy from its unstrained value to:

$$E(\delta) = E(-\delta) = E(0) + (C_{11} - C_{12}) V\delta^2 + O\left(\delta^4\right) \quad (3)$$

where E_0 is the energy of the unstrained lattice, V is the unit cell volume and δ is the strain parameter. $O(\delta^4)$ means ignoring the power higher than 4. For the elastic modulus C_{44}, we used the volume-conserving monoclinic strain tensor

$$\begin{bmatrix} 0 & \dfrac{1}{2}\delta & 0 \\ \dfrac{1}{2}\delta & 0 & 0 \\ 0 & 0 & \dfrac{\delta^2}{4-\delta^2} \end{bmatrix} \quad (4)$$

which changes the total energy to:

$$E(\delta) = E(-\delta) = E(0) + \frac{1}{2}C_{44}V\delta^2 + O\left(\delta^4\right) \quad (5)$$

For an isotropic cubic, the bulk modulus is given by:

$$B = \frac{1}{3}(C_{11} + 2C_{12}) \quad (6)$$

The values of C_{11}, C_{12}, and C_{44} are calculated for ZB MnSb as 45.60, 31.37, and 29.48 GPa, respectively. It is also shown that $(C_{11} - C_{22}) \succ 0$ could be a signal for elastic stability of ZB MnSb. To our knowledge the elastic constants of ZB structure for MnSb have not yet been measured or calculated.

B. Interface properties of MnSb/GaSb(001)

1. Structural properties of MnSb/GaSb(001) interface

A practical approach for stabilizing MnSb compound in the metastable ZB structure is the pseudomorphic growth of MnSb thin film on a ZB semiconductor. In this regard, GaSb semiconductor with ZB stable structure is a promising candidate due to its close lattice matching to ZB MnSb. The experimental lattice constant of GaSb, 11.74 Bohr, is close to the theoretical lattice parameter of ZB MnSb, 11.69 Bohr within GGA. Moreover, the presence of the Sb element at both sides of the MnSb/GaSb(001) interface enhances the possibility of a successful pseudomorphic epitaxial growth of this heterostructure. We adopted the GGA theoretical value (11.69 Bohr) for interface calculations, which has a few mismatch with GGA lattice parameter of ZB MnSb.

This lattice mismatch induces a low biaxial strain in the deposited MnSb thin films on GaSb(001) substrate. In order to understand the influence of this biaxial strain on the electronic properties of MnSb thin films, we studied the isotropically compressed and tetragonally distorted ZB structure of bulk MnSb. The former structure is a ZB lattice at theoretical lattice parameter of GaSb while the latter is a tetragonal structure in which the in-plane lattice parameters are set to be GaSb lattice constants. The vertical lattice parameter is also relaxed to minimum total energy. We have optimized the interfacial distance parameter (the spacing between substrate and film) by testing different values of these parameters. We have also let atoms move along [001] to minimize the total energy and the force acting on atoms simultaneously.

For MnSb/GaSb(001) interface calculations, we applied slab supercells consisting of 8 atomic monolayers for both GaSb (substrate) and MnSb (film), stacked along (001) direction. The investigated junctions for MnSb/GaSb(001) is .../Ga/Sb/Mn/.... The in-plane lattice parameters are set equal to GaSb lattice parameters (11.74 Bohr). All structural parameters of the interface supercell, including interlayer and interface distances and atomic positions were accurately relaxed and optimized. Here we give several interlayer distances in the relaxed Sb terminated GaSb/MnSb(001) interface $d^i_{\mathrm{Sb-X}}$, the index i measures from both sides the distance from the interface, i=0 indicates the distance between the interface Sb and subinterface Mn or Ga layers. $d^2_{\mathrm{Ga-Sb}}$, $d^1_{\mathrm{Ga-Sb}}$, $d^0_{\mathrm{Ga-Sb}}$, $d^0_{\mathrm{Mn-Sb}}$, $d^1_{\mathrm{Mn-Sb}}$, $d^2_{\mathrm{Mn-Sb}}$, is 2.89, 2.92, 2.96, 2.84, 2.85, 2.88 Å, respectively. The bulk values of $d^{\mathrm{bulk}}_{\mathrm{Ga-Sb}}$ and $d^{\mathrm{bulk}}_{\mathrm{Mn-Sb}}$ are 2.90 and 2.88 Å, which indicates that Ga-Sb interlayer distance at the interface is slightly increased compared to the bulk value while the interface Sb-Mn interlayer distance will be decreased. On the other hand, the interface Mn atom is slightly displased toward neighbouring Mn atom, indicating further tendency of Mn atom (compared with Ga) to make bond with Sb atom.

2. Electronic properties of MnSb/GaSb(001)

To investigate the electronic structure of MnSb/GaSb(001) interface, the atomic partial DOS of several layers were calculated.

The total DOS of MnSb/GaSb(001) is shown in Fig.2(a). It can be seen from this figure that the half-metallic property is preserved. We also conclude from Fig.2(a) that the 100% spin polarization exists at Fermi level. Figure 2(b) shows that the Ga atoms in sub-interface layer will have the half-metallic property with the energy gap at spin down. In Fig.2(c) it is shown that the Ga atoms in central layers have a bulk like nonmagnetic DOS with a clear band gap at Fermi level. Also in

DOI:10.1088/1674-0068/24/02/155-161 ©2011 Chinese Physical Society

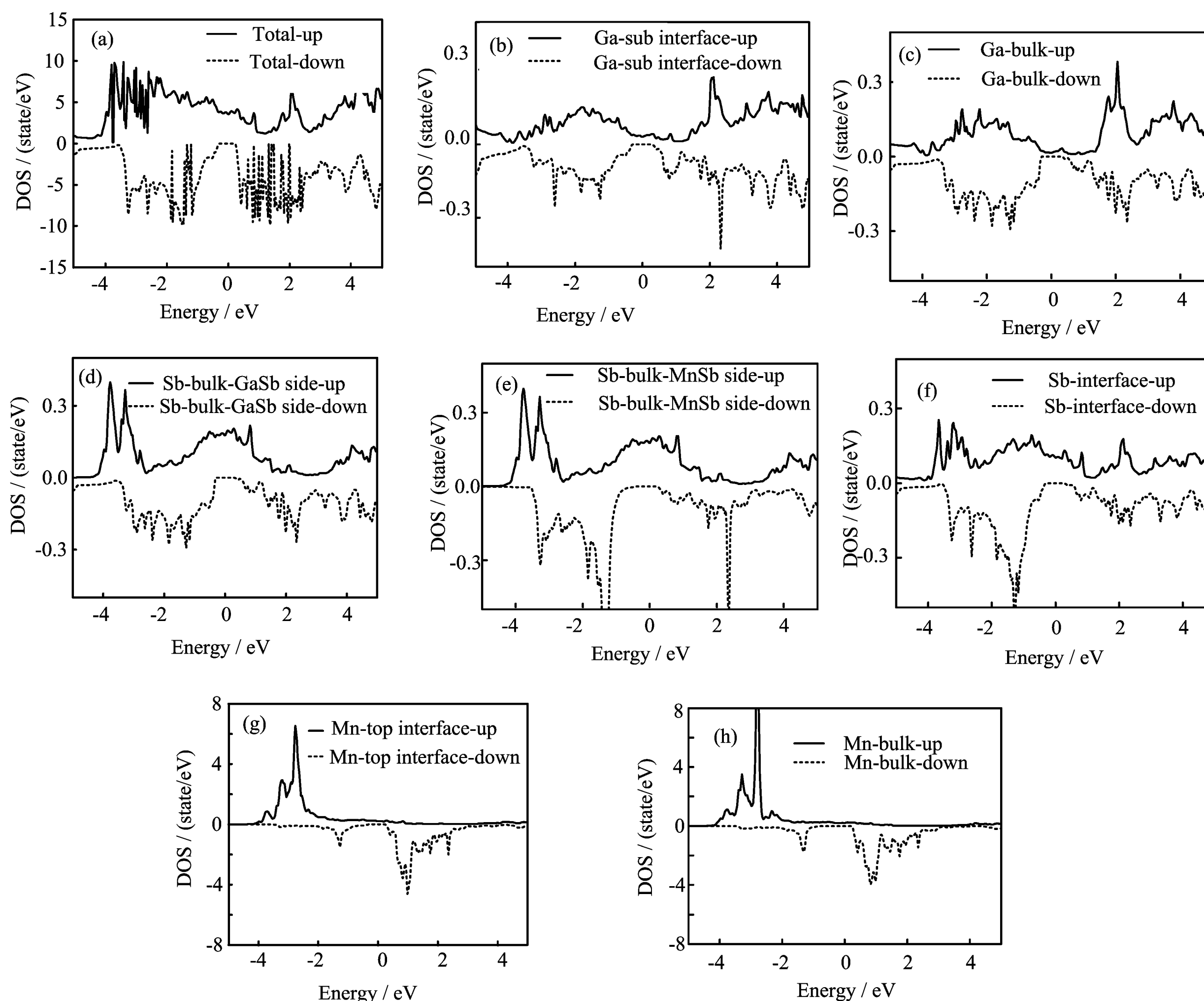

FIG. 2 The spin polarized atomic DOS at various layers of the MnSb/GaSb(001) interface supercell.

Fig.2 (d), (e), and (f) we see the half-metallic property in the Sb layers at central substrate (GaSb), central film (MnSb) and the interface. As it can be seen from Fig.2 (d), (e), and (f), the magnitude of DOS is reduced at the Fermi level in comparison to bulk states. In addition the states of electrons at interface shifted to the Fermi level. Figure 2 (g) and (h) indicate the half-metallic property of Mn atoms at both top-interface layer and central MnSb film.

By approaching the interface the nonmagnetic partial DOS at GaSb substrate continuously change toward the ferromagnetic half-metallic behaviour in MnSb film in such a way that the interface Sb atom exhibits a moderate exchange splitting. The Sb atoms at interface layer connect the nonmagnetic Ga slab to the ferromagnetic Mn layers. The p-d hybridization between Sb and Mn at interface enhances the exchange interactions in the interface Sb while the s-p hybridization between interface Sb and Ga substrate weakens the exchange interaction. Therefore the interface Sb atoms have a medium behavior between Sb atoms in the bulk MnSb and GaSb. It is also seen that the partial DOS of the interface Sb and Mn are more broadened than the central Sb and Mn partial DOS, which could be a signal for stronger Mn-Sb interaction at interface. Another conclusion to be drawn is that the DOS in both majority and minority channels are shifted away from the Fermi level in comparison with the bulk Mn like states. This is due to the potential difference between the semiconductor and half-metal sides of the interface.

The band structure of MnSb/GaSb(001) is shown in Fig.3. The bands around -10 eV are mainly due to the semi-core Sb s states being well separated from the valance bands. It can also be seen that there is a direct energy gap in Γ direction. The broadening of bands for up spin is more than the broadening of bands for down spin. In Fig.3(a) the bands in the region from -4 eV to -2 eV belong to Mn d orbital whereas the Fermi surface bands belong to Sb p. In the Fig.3(b) the Mn d bands in down spin are shifted to 1 eV region and Sb

DOI:10.1088/1674-0068/24/02/155-161 ©2011 Chinese Physical Society

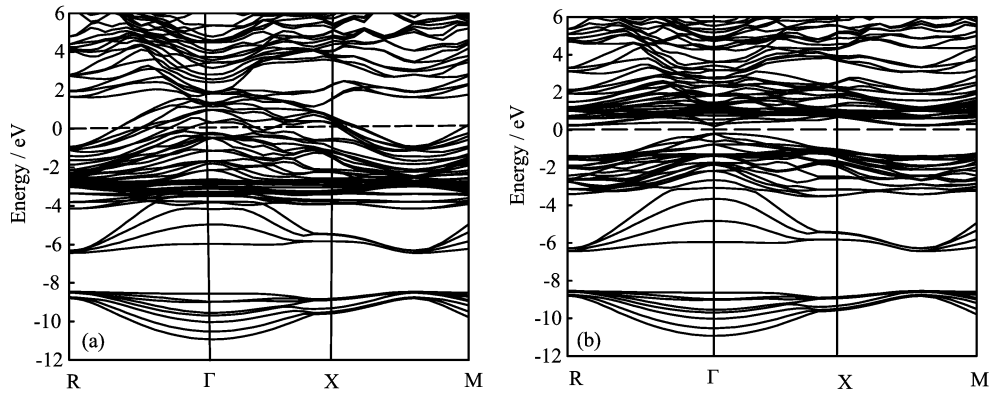

FIG. 3 The majority (a) and minority (b) electronic band structure of MnSb/GaSb(001) interface. The Fermi energy is set to zero.

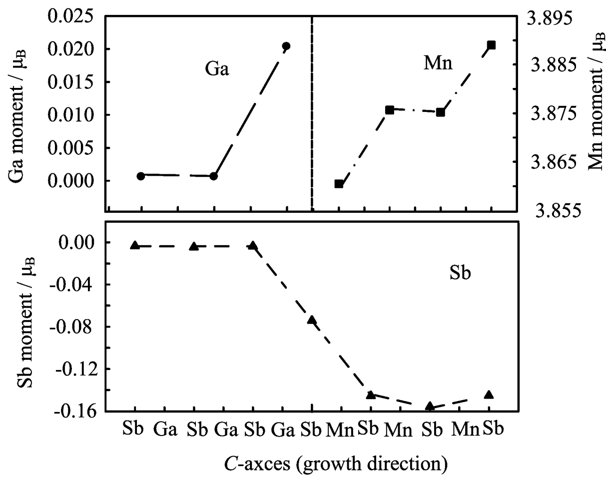

FIG. 4 The local atomic magnetic moments plotted as a function of layer distance to the interface. The interface Sb layer is shown by dotted line.

p bands are localized in the region of from −4 eV to −2 eV.

3. Magnetic properties of MnSb/GaSb(001) interface

In Fig.4, we have plotted the magnetic moments of different atomic species in the MnSb/GaSb(001) junction as a function of distance from the interface. It is important to note that, sufficiently far from the junction, the bulk magnetic moments are recovered. The bulk values for Mn and Sb atoms in the strained MnSb compound are 3.89 and −0.14 μ_B while GaSb is a nonmagnetic semiconductor with zero atomic magnetic moment. The magnetic moment of the interface Sb atom is equal to the average of the corresponding bulk values in two sides of the interface, consistent with the intermediate character of interface Sb atom observed in the DOS plots. By approaching the interface, the magnetic moment of Mn decreases while that of Ga atom slightly increases. The origin of this behavior is the hybridization of the ferromagnetic MnSb layers with nonmagnetic GaSb layers at the interface.

4. Band alignment

The spin resolved band alignment parameters are technologically relevant quantities in the electronic transport properties of layered devices. In general a half-metal/semiconductor heterojunction for the majority spin resembles a metal/semiconductor contact with a p- or n-type Schottky barrier (Φ_p, Φ_n) while in the minority channel this interface acts as a semiconductor/semiconductor heterojunction and the band discontinuities are defined as the valence and conduction band offsets (VBO, CBO). Φ_p and Φ_n are defined as the difference between semiconductor valence band maximum, VBM, (conduction band minimum, CBM) and metal Fermi level while VBO (CBO) is the difference between minority half-metal VBM (CBM), and semiconductor VBM (CBM). In order to calculate the band alignment parameters we follow the established "bulk plus line up" procedure in which the bulk band structures are combined with a potential line up parameter obtained from interface slab calculation. The potential line up at GaSb/MnSb(001) heterojunction is determined by comparing the electronic structure of the core electrons in the bulk and interface central layers. The 1s core electrons are selected for this purpose as they are well shifted from the interface effects. The potential line up parameter is defined as: $\Delta E_s^{\text{bulk}} - \Delta E_s^{\text{slab}}$, where ΔE_s^{bulk} and ΔE_s^{slab} are the energy difference of Mn1s and Ga1s core electrons in the bulk compounds and slab central layers, respectively. In this sence a potential line up of about 0.16 eV was obtained for the Sb terminated GaSb/MnSb(001) interface. By applying this potential line up, we aligned and matched separately calculated bulk band structure of MnSb with GaSb to determine the band diagram of GaSb/MnSb(001) heterojunction, presented in Fig.5. The well-known deficiency

DOI:10.1088/1674-0068/24/02/155-161 ©2011 Chinese Physical Society

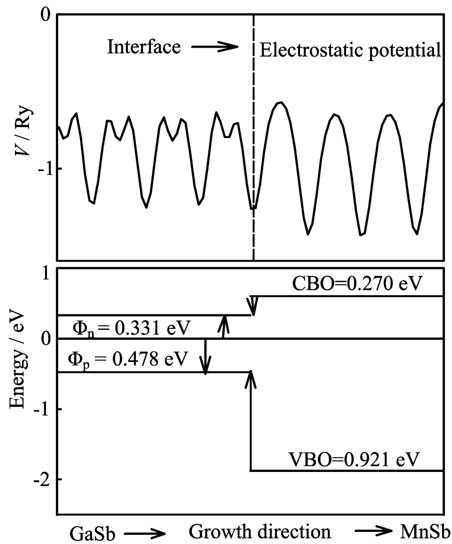

FIG. 5 The schematic electrostatic potential and band diagram at MnSb/GaSb(001) heterojunction. The MnSb Fermi energy is set to zero.

LDA/GGA studies in determination of the semiconductor band gaps induce substantial error in the position of GaSb CBM. Hence, in order to solve this problem and obtain reliable band alignment parameters, we shifted up the GaSb CBM to recover the experimental band gap value (0.726 eV).

The obtained band alignment parameters in MnSb/GaSb(001) interface are listed in Table II in order to compare with pervious reported data for other interfaces. The contribution of minority electrons of binary ZB half-metals in injected currents could lead to more efficient spin injection into semiconductors. As it can be seen from the Fig.5, the Fermi level of MnSb lay below the CBM of GaSb semiconductor. This indicates that Schottky barrier can be formed for n-GaSb and a reverse bias should be applied in order to allow majority spin to tunnelling into GaSb semiconductor. Figure 5 also shows that the CBM of minority spin in the MnSb lies at about 0.27 eV above the CBM of GaSb and so the majority spin electrons can be directly injected to n-GaSb. In other word the probability of electrons being flipped to the CBs of minority spin under the applied reverse bias are decreased. This could be a signal for possibility of highly efficient spin injection.

IV. CONCLUSION

In this work, density functional-full potential computations were employed to investigate the structural, electronic and magnetic properties of bulk MnSb phases and MnSb/GaSb(001) interfaces. We concluded that NiAs structure is more stable than ZB structure in equilibrium volume and it is clearly seen that the NiAs structure is less compressible than the other compounds. It was also seen that at MnSb/GaSb(001) interface, the electronic and magnetic properties of atomic layers changed coherently from nonmagnetic semiconductor substrate to ferromagnetic half-metallic film. Results of our calculations indicates that MnSb retain Half-metallic behavior at MnSb/GaSb(001) interface. The DOS of Sb interface atoms in MnSb/GaSb(001) heterojunction shows an intermediate behavior in comparison with central atoms of film and substrate. The calculated band alignment at MnSb/GaSb(001) heterojunction shows the possibility of directly injecting majority of being flipped to the CBs of the minority spin of MnSb. Finally it was found that the MnSb/GaSb(001) heterojunction has a substantially higher minority valence band offset compared with Husler based heterojunction .

TABLE II The majority Schottky barrier (eV) and minority band offsets (eV) at MnSb/GaSb(001) heterojunction. Our results are compared with the band alignment parameters of some other half-metal/semiconductor heterojunction.

Heterojunction	Φ_n	Φ_p	VBO	CBO
MnSb/GaSb (this work)	1.24	0.51	1.25	0.47
CrSe/ZnSe [28]	1.84	0.88	1.94	1.28
VAs/GaAs [29]	1.19	0.23	1.03	0.93
Co_2MnSi/GaAs [30]	1.20	0.18	0.03	0.50
$Co_2Cr_{0.5}Fe_{0.5}Al$/GaAs [31]	2.20	−0.78	0.32	1.39

[1] M. N. Biabich, J. M. Broto, A. Fert, and Van. Nguyen, Phys. Rev. Lett. **61**, 2472 (1988).
[2] G. Binasch, P. Grünberg, F. Saurenbach, and W. Zinn, Phys. Rev. B **39**, 4828 (1989).
[3] G. Schmidt, D. Ferrand, L. W. Molenkamp, A. T. Filip, and B. J. van Wees, Phys. Rev. B **62**, R4790 (2000).
[4] H. J. Zhu, M. Ramsteiner, M. Wassermeier, and H. P. Schönherr, Phys. Rev. Lett. **87**, 016601 (2001).
[5] R. De Groot, F. M. van Engen, and P. G. van Engen, K. Buschow, Phys. Rev. Lett. **50**, 2024 (1983).
[6] Y. Onhno, D. K. Young, B. Beschoten, F. Matsukara, H. Ohno, and D. D. Awschalom, Nature **402**, 790 (1999).
[7] R. J. Soulen Jr., J. M. Byers, M. S. Osofsky, B. Nadgorny, T. Ambrose, S. F. Cheng, P. R. Broussard, C. T. Tanaka, J. Nowak, J. S. Moodera, A. Barry, and J. M. D. Coey, Science **282**, 85 (1998).
[8] J. H. Park, E. Vescovo, H. J. Kim, C. Kwon, R. Ramesh, and T. Venkatesan, Nature (London) **392**, 794 (1998) .
[9] I. Galanakis, S. Ostanin, M. Alouani, H. Dreyssé, and J. M. Wills, Phys. Rev. B **61**, 4093 (2000).
[10] (a0 G. A. Wijs and R. A. de Groot, Phys. Rev. B **64**, R020402 (2001).
(b) I. Galanakis, J. Phys: Condens. Matter. **14**, 6329 (2002).

DOI:10.1088/1674-0068/24/02/155-161 ©2011 Chinese Physical Society

[11] (a) D. Ristoiu, J. P. Nozieres, C. N. Borca, T. Komesu, H. K. Jeong, and P. A. Dowen, Europhys. Lett. **49**, 624 (2000).
(b) D. Ristoiu, J. P. Nozières, C. N. Borca, B. Borca, and P. A. Dowben, Appl. Phys. Lett. **76**, 2349 (2000).

[12] K. Ono, J. Okabayashi, M. Mizuguchi, M. Oshima, A. Fujimori, and H. Akinaga, J. Appl. Phys. **91**, 8088 (2002) .

[13] H. Akinaga, T. Manago, and M. Shirai, Jpn. J. Appl. Phys. Part 2 **39**, L1118 (2000).

[14] M. Mizuguchi, H. Akinaga, T. Manago, K. Ono, M. Oshima, M. Shirai, M. Yuri, H. J. Lin, H. H. Hsieh, and C. T. Chen, J. Appl. Phys. **91**, 7917 (2002).

[15] J. H. Zhao, F. Matsukura, T. Takamura, D. C. E. Abe, and H. Ohno, Appl. Phys. Lett. **79**, 2776 (2001).

[16] M. G. Sreenivasan, X. J. Hou, K. L. Teo, M. B. A. Jalil, T. Liew, and T. C. Chong, Thin Solid Films **505**, 133 (2006).

[17] M. G. Sreenivasan, J. F. Bi, K. L. Teo, and T. Liew, J. Appl. Phys. **103**, 043908 (2003).

[18] J. E. Pask, L. H. Yang, C. Y. Fong, W. E. Pickett, and S. Dang, Phys. Rev. B **67**, 224420 (2003).

[19] M. S. Miao and Walter R. L. Lambrecht, Phys. Rev. B **71**, 064407 (2005).

[20] Y. Q. Xu, B. G. Liu, and D. G. Pettifor, Phys. Rev. B **66**, 184435 (2002).

[21] S. A. Hatfeild and G. R. Bell, J. Cryst. Growth **296**, 165 (2006).

[22] R. X. Dai, N. F. Chen, X. W. Zhang and T. P. Chang, J. Cryst. Growth **299**, 142 (2007).

[23] P. Blaha, K. Schwarz, P. Sorantin, and S. B. Trickey, Comput. Phys. Commun. **59**, 399 (1990).

[24] J. Perdew, K. Burke, and M. Ernzerhof, Phys. Rev. Lett. **77**, 3865 (1996).

[25] I. Galanakis and P. Mavropoulos, Phys. Rev. B **67**, 104417 (2003).

[26] M. J. Mehl, Phys. Rev. B **47**, 493 (1993).

[27] M. J. Mehl, J. E. Osburn, D. A. Papaconstantopoulos, and B. M. Klein, Phys. Rev. B **41**, 10311 (1990) .

[28] E. Hazrati, S. J. Hashemifar, and H. Akbarzadeh, J. Appl. Phys. **104**, 113719 (2008).

[29] R. Q. Wu, G. W. Peng, and Y. P. Feng, J. Phys. Conference Series **29**, 150 (2006).

[30] N. Ghaderi, S. Hashemifar, H. Akbarzadeh, and M. Peressi, J. Appl. Phys. **102**, 074306 (2007).

[31] S. Zarei, S. J. Hashemifar, H. Akbarzadeh, and Z. Haffari, J. Phys.: Condens. Matter. **21**, 055002 (2009).

DOI:10.1088/1674-0068/24/02/155-161
©2011 Chinese Physical Society